Supplementary Materials for

Simoni, A; Wolfgang, W; Topping, MP; Kavlie, RG; Stanewsky, R; Albert, JT; (2014) A mechanosensory pathway to the Drosophila circadian clock. Science , 343 (6170) 525 - 528. 10.1126/science.1245710.

Correspondence to: r.stanewsky@ucl.ac.uk or joerg.albert@ucl.ac.uk

This PDF file includes:

Materials and Methods

Flies

CantonS and *per*^{01} *(10)* flies were used as controls. *per*^{01}*; 13.2* flies *(11, 12)* carry a genomic *per* rescue construct (on chromosome 3). *tilB*^{1} and *nocte*^{P} flies have been described previously *(2, 11)*. For the antennal-ablation experiments, adult flies were anaesthetized under CO_2 and the antennae were manually ablated using sharp forceps. All three antennal segments were removed. Ablation was performed before loading the flies into the behavior monitor.

Bioluminescence readings

For this experiment we used the previously described (*8, 15*) *per*-insertion line *8.0-luc:9*, which expresses a PER:LUC fusion protein in subsets of clock neurons, and thus allows for monitoring the free-running oscillations of PERIOD protein levels in central clock neurons, which is not possible using PER-LUC reporters that are expressed more widely (i.e. in all clock gene expressing cells) because of the resulting rapid damping of oscillations. For each bioluminescence experiment, male flies were initially exposed to 12h:12h LD cycles for 3 days and then kept in DD. Relative to the previous light onset, the 12h:12h VS cycles were started 6h earlier (advance experiments) or 6h later (delay experiments). VS cycles lasted 5 days. In the last silent phase, VS and silent control flies were simultaneously anesthetized with diethylether (< 5 sec) and transferred individually to wells of 96-well micro titer plates under safe light. Wells contained luciferin-fortified food, and were measured hourly in DD and 21°C for 5 days (the 1st three days are shown in Fig. 3 and the 1st five days in Fig. S8) using a TopCount plate reader (Perkin-Elmer) as previously described (*12*). For delay experiments the transfer was done at ZT20 and for advance experiments at ZT8, relative to the previous vibration onset.

All bioluminescence data were de-trended and normalized in a three step process (see Figure S8):

(I) a cubic polynomial, $y = y_0 + ax + bx^2 + cx^3$, was fitted to the raw data (baseline determination)

(II) the local y-values of the curve fit were subtracted from each raw data point (baseline subtraction) and the resulting, baseline-corrected, data was then fitted with a sinusoidal model, $y = A\sin\left(\frac{2\pi t}{\tau} + \phi\right)$, with A being the sine wave amplitude, t being the time point, τ being the sine wave period and ϕ being the sine wave phase. (III) both sinusoidal fits and corresponding baseline-corrected data were normalized to the maximum of the fit function, to highlight phase differences.

Activity Monitoring

Locomotor activity rhythms were recorded automatically using the *Drosophila* Activity Monitoring (DAM) system (Trikinetics, Waltham, MA) as previously described (*14*). Flies were kept in glass tubes supplemented with 5% Sucrose and 2% agar and entrained to 12h:12h LD cycles at 21°C, followed by the respective experimental conditions (see text and Figure legends). Data analysis was performed with Matlab and fly toolbox library functions (*9*). Locomotor activity rhythms were recorded automatically using the *Drosophila* Activity Monitoring (DAM) system (Trikinetics, Waltham, MA) as previously described (*14*).

Phase analysis

For each fly of a given group (exposed to VS or silent control), the average estimate of peak phase for each fly for 3 to 4 consecutive days in the final free running condition is plotted as a point on a unit circle. Phase 0 corresponds to stimulus on, in this case vibration on. A mean vector, extending from the center of the unit circle towards the diameter is calculated for each group of flies exposed to the same condition; the direction of the vector indicates mean peak phase for the entire group and the length of the vector represents the phase coherence of the group between the points. The internal black circumference represents 100% coherence between individuals of the same group. Thus, in the extreme, if all the points were uniformly dispersed around the circle, the magnitude of the vector would be zero; whereas if they all occurred precisely in the same location, the magnitude of the vector would be 1. The two average vectors are compared and an F-statistic (Watson-Williams-Stevens test) is calculated to evaluate whether the mean phase vectors are significantly different from one another. The average phase difference between the two groups is given in [h]. Red circles indicate phase of flies exposed to vibration stimulus, and gray stars refers to silent control.

Generation, monitoring and structure of the mechanical stimulus

In order to record the flies' locomotor activity in response to 12h:12h vibration:silence (VS) cycles, the *Drosophila* activity monitors (DAMs) were mounted on top of the frame of a 381 mm bass loudspeaker (Delta15, Eminence Speaker LLC). Movements between loudspeaker and monitors were restricted by using strong double adhesive tape connecting the activity monitor to the loudspeaker frame. With this arrangement, loudspeaker activity led to up-and-down movement of the activity monitor, i.e. movement perpendicular to the loudspeaker membrane. This vertical movement of the DAMs was recorded and the recordings were used to monitor the mechanical stimulus during the course of an experiment and to adjust the stimulus to equal intensities in between different experiments. Stimuli were generated by the graphical stimulus sequence editor of the Spike2 software (Cambridge Electronics Design) and played to the loudspeaker via a D/A converter (Micro 1401-3, Cambridge Electronics Design). The looped stimulus sequence consisted of a 12h period in which vibrations were applied followed by a 12h period of silence. During the 12h of silence, no stimulus was provided. During the 12h of vibration, a 0.5s long 40Hz vibration alternated with a 0.5s long 200Hz vibration with a 0.5s long gap of silence in between them (see Fig. 1B). Both 40Hz and 200Hz vibrations were manually adjusted to velocity amplitudes of ~20mm/s thus providing a vibratory stimulus that could be expected to stimulate ChOs in both legs and antennae (*3, 26*). Centering the stimuli around equal velocities (~20mm/s) made sure that the magnitudes of the remaining two principal components (displacement and acceleration) were large enough to fall within the ranges of reported ChO sensitivities (*3*). Playing the two stimulus frequencies of 40Hz and 200Hz separately improved reproducibility and calibration of the stimulus and avoided any nonlinear interaction (distortion) within the loudspeaker. Exposure to constant vibrations (VV) did not interfere with normal circadian behavior. Exposure to 12h:12h LD cycles in VV (LD-VV) resulted in close-to-normal entrainment and sustained rhythmicity in subsequent exposure to DD-VV (Fig. S9). All tested genotypes showed a significant increase of their locomotor activity at the onset of the first presented vibration ($p<0.001$ in all cases; Fig. S1), demonstrating perceptibility of the vibratory stimulus. This onset response was reduced in mutants known to impair ChOs, demonstrating the contribution of ChOs to stimulus perception (Fig. S1).

Recordings of DAM movements were carried out with a piezoelectric charge accelerometer (Type 4370, Brüel & Kjaer), which was mounted, via a magnetic connector, to a metallic plate glued on the DAM. The accelerometer signal was fed into a charge conditioning amplifier (Type 2635, Brüel & Kjaer) and the amplified signal was digitized at a sampling rate of 1.25 kHz using an A/D converter (Micro 1401-3, Cambridge Electronics Design).

Temperature Monitoring

In order to be able to monitor the flies' effective ambient temperatures continuously throughout the experiments, we fitted a K-type thermocouple (sensor size <4mm) into one of the behavioral tubes. The sensor was connected to a Type K Thermocouple Amplifier (Analog Devices AD595). The system converted the temperature in the behavioral tubes to a voltage signal with a proportionality coefficient of 100mV/°C. The voltage signal was then digitized at a sampling rate of 2 Hz using an A/D converter (Micro 1401-3, Cambridge Electronics Design) and recorded in parallel to the vibrational data. Data analysis was carried out using the Spike2 software (Cambridge Electronic Design). No diurnal temperature oscillations were observed in any of the experiments (see Fig. S10 for an example). As a precautionary measure, though, experiments in which the difference between the lowest and the highest recorded temperature exceeded 1.5°C for any of the experimental days were excluded from the analysis. The average temperature during the vibration/silence entrainment experiments was 21.4°C±1.2°C (across 19 experimental runs).

Entrainment index

The Entrainment Index (EI), was calculated as described in ref. (*8*). EI is the ratio of the total average activity of a particular genotype during the 4 hr before the vibration stimulus onset (ZT20-24) over the activity of the silent phase (ZT12-24) for the last three days of the VS2 part of the experiment. The activity window does not include the transition points (vibration-on and vibration-off) in order to avoid the startle responses which could affect the EI value due to masking effects (i.e. EI reflects true entrainment). A one-way ANOVA analysis with uncorrected Fisher's Least Significance Difference test was used to determine significant difference between genotypes. Analysis performed with GraphPad Prism 6.

Magnetic field fluctuations

Flies have previously been reported to be able to synchronize their locomotor behavior to diurnal fluctuations of the surrounding electromagnetic field. This magnetosensitive behavior was shown to use a cryptochrome- and light-dependent sensory pathway (*27, 28*). A priori, it could not be excluded that a loudspeaker-based vibration paradigm such as the one used in this study leads to magnetic field fluctuations around the flies' behavioral tubes strong enough to affect the flies' locomotor behavior. Using an Electromagnetic Field (EMF) Tester (EMF-822A, Lutron Electronic Enterprise) we therefore recorded the EMF strengths that occurred around the activity monitors during the vibration and silent phases. The maximum field strengths at the level of the behavioral tubes that were recorded during the vibration phase (loudspeaker ON) were ~16 µT. The baseline field strengths during the silence phase (loudspeaker OFF) were ~0.08µT - 0.16µT. The maximal magnetic field strength values that accompanied the diurnal pattern of vibration and silence were thus about one order of magnitude smaller than those shown to affect the flies' circadian clock (*28*). Moreover, magnetosensitivity in flies has been shown to be light-dependent (*27, 28*). All mechanical entrainment experiments however were carried out in complete darkness. An experimental distortion of the mechanical entrainment by concomitant magnetic field fluctuations can thus be excluded.

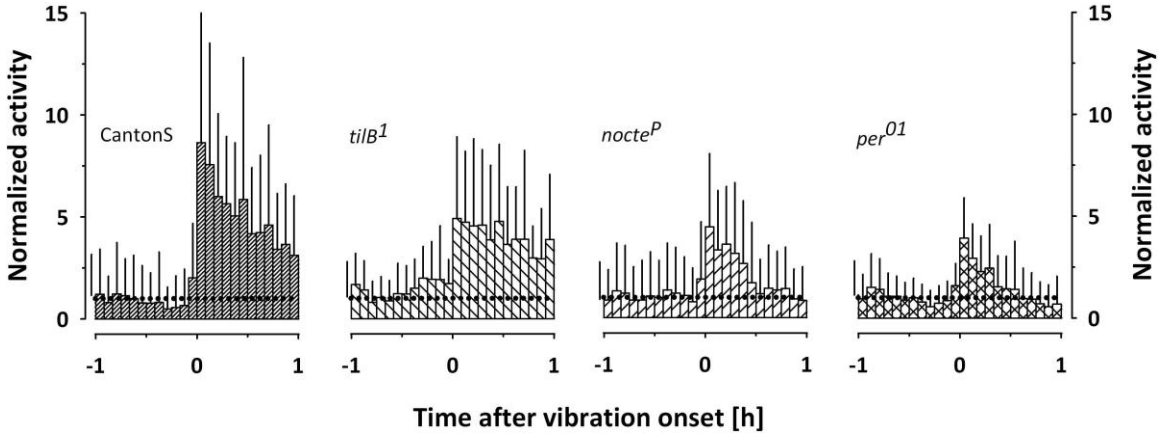

Fig. S1. Direct locomotor responses to the vibratory stimulus for wildtype and mutant flies. Shown are the normalized locomotor responses to the first presentation of the vibratory stimulus (at the start of VS1). In order to allow for a direct comparison between the different genotypes, locomotor activities were normalized to the average values displayed by each genotype during the hour directly preceding stimulus onset (i.e. baseline activity=1, dotted line). All genotypes showed a significant increase of locomotor activity immediately after vibration onset (CantonS: P<0.001, n=47; *tilB*^{1}: P<0.001, n=16; *nocte*^{P}: P<0.001, n=45; *per*^{01}: P<0.001, n=25; Mann-Whitney Rank Sum Test) demonstrating general perception of the stimulus. As compared to CantonS wildtype flies, the responses of the chordotonal mutants *tilB*^{1} and *nocte*^{P} were significantly reduced (*tilB*^{1}: P=0.031, *nocte*^{P}: P=0.001), suggesting that signaling by chordotonal organs contributes to the animals' responses. Note that locomotor responses were also significantly reduced in clock mutant flies (*per*^{01}: P=0.003). Error bars represent SD.

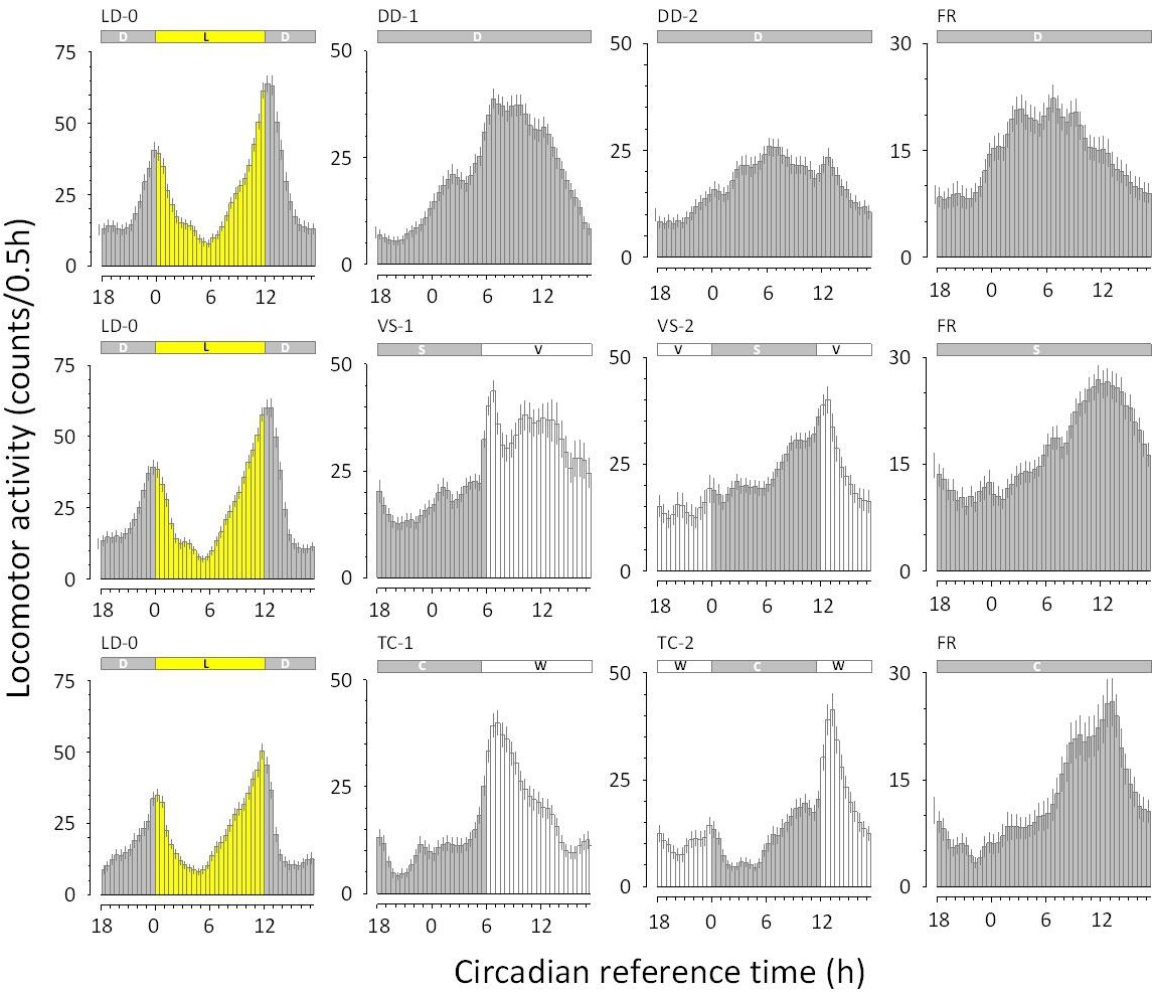

Fig. S2. Behavioral synchronization by Vibration/Silence (VS) cycles shares similarities with temperature cycle (TC) entrainment. (**Top**) control flies (CantonS, n=72), which were kept in DD before the final free run (LD→DD→DD→FR), (**Middle**) experimental flies (CantonS, n=75) subjected to VS entrainment (LD→VS1→VS2→FR), (**Bottom**) experimental flies (CantonS, n=25) subjected to 12 hr: 12 hr (16°C: 20°C) TC entrainment (LD→TC1→TC2→FR) (all data re-plotted from Fig. 1 and ref. (*29*)). Note that in FR the peak activity phases of both lines of experimental flies differ from those of control flies and that they have been shifted similarly in VS and TC entrained flies. All experimental stages, except the initial LD entrainment, took place in complete darkness. Error bars represent SEM.

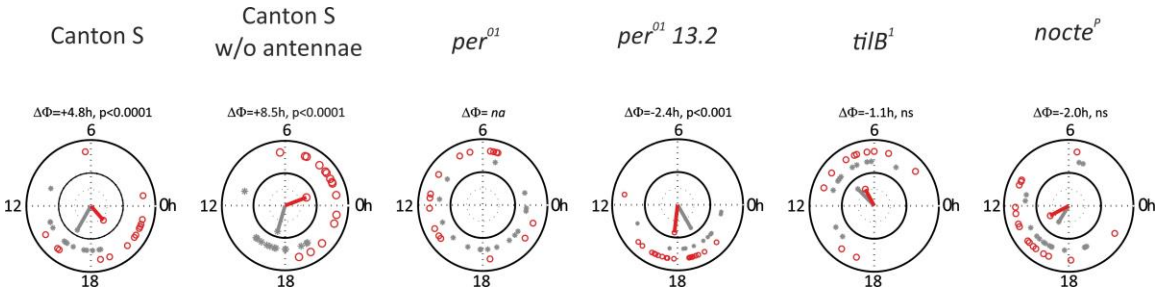

Fig. S3. Circular phase analysis of individual experiments for final 5 days in free-running (FR) conditions of experimental flies exposed to VS cycles (red circles) and control flies not exposed to VS cycles (grey asterisks). See refs. (*7, 9, 10*) for details on circular plots, phase analysis and statistics used.

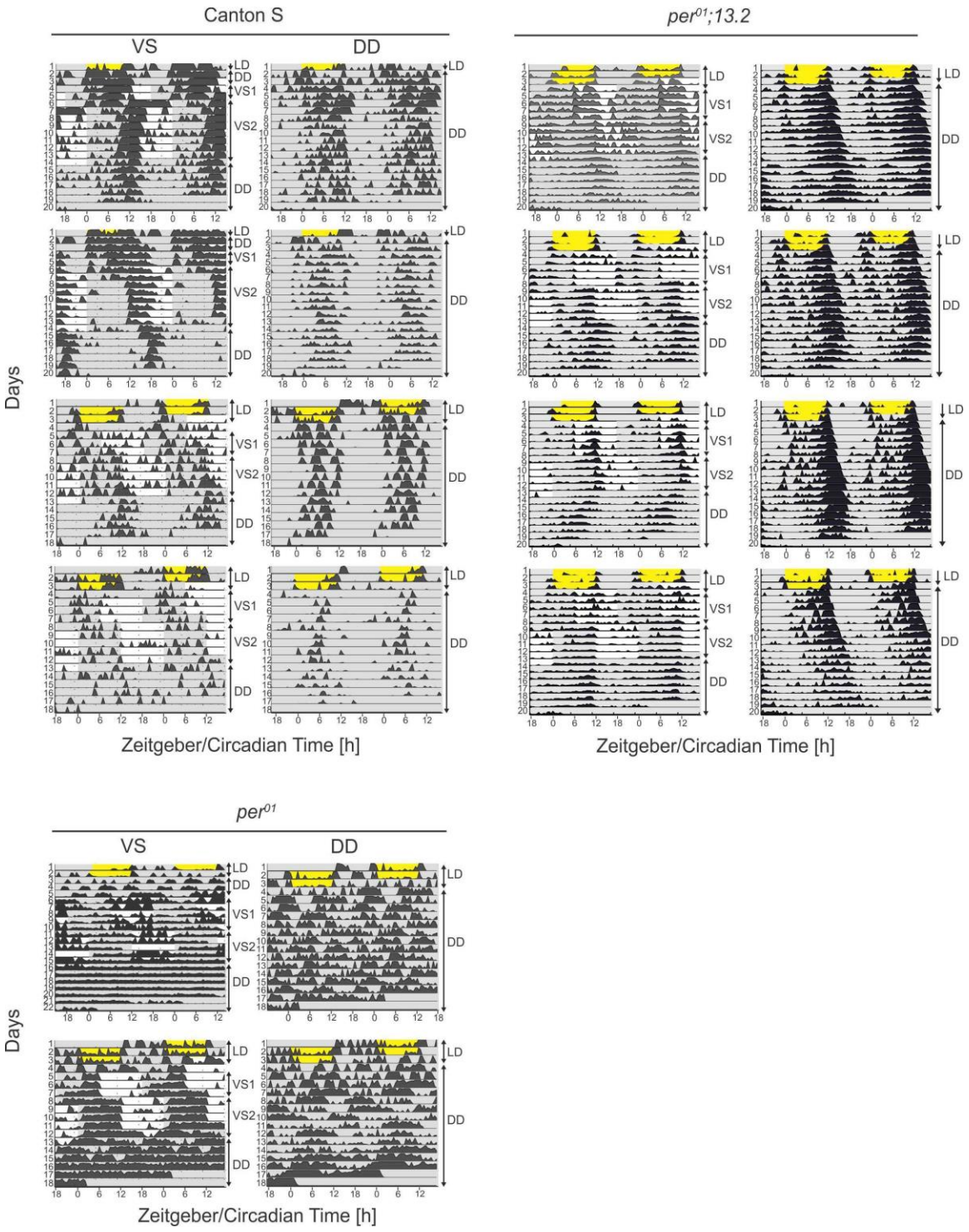

Fig. S4. Individual records of wildtype, *per*^{01}, and *per*^{01} *13.2* flies before, during, and after mechanical stimulation. Individual actograms of flies exposed to the same VS conditions as in Fig. 1B are shown in the left columns (VS), controls not exposed to VS cycles in the right columns (DD) of each genotype. The upper 3 rows of CantonS and *per*^{01} *13.2* show flies that were classified as 'synchronized' based on their behavior during and after the VS cycles. They adjust their behavioral activity peaks to occur at the beginning of each V phase and this pattern is maintained after transition

to constant conditions, indicating stable entrainment. Row four shows an example of a fly classified as ‘not-entrained‘ for both genotypes. For *per*^{01} two flies with opposite behavior during the V-part of the VS cycle are shown (active and inactive, respectively). Note that most of the *per*^{01} flies were inactive during the V phase (see Fig. S6). Actogram shading as in Fig. 1C: Grey areas: darkness, yellow areas: light, white areas: vibration in darkness.

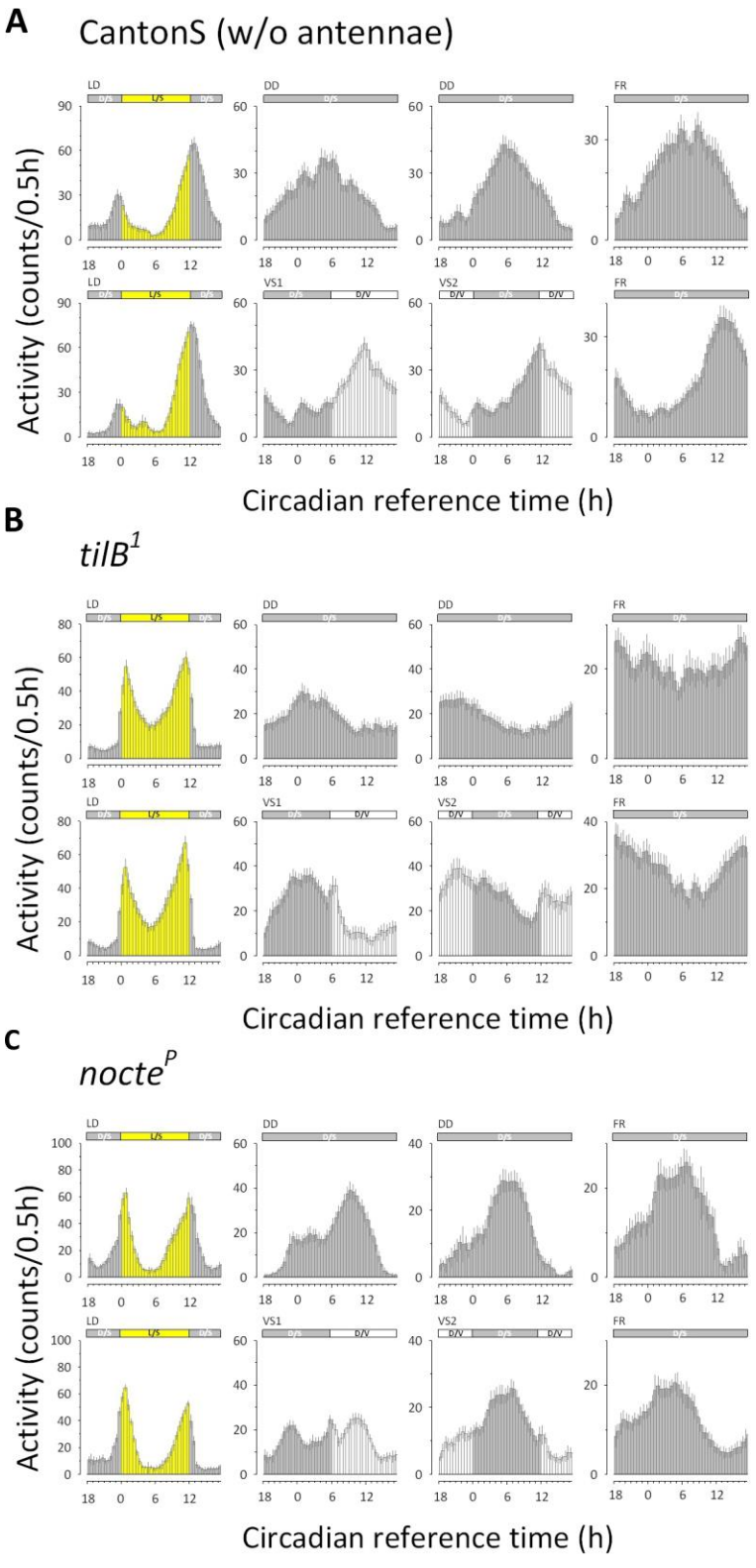

Fig. S5. Histograms showing the daily average activities of control flies (top row in each panel) and experimental flies (bottom row in each panel) during different phases of the entrainment regime (nomenclature from main text). (**A**) antenna-ablated CantonS wildtype flies (n=28, vibrated; n=30, FR), (**B**) *tilB*^{1} mutant flies (n=24, vibrated; n=25, FR) and (**C**) *nocte*^{P} mutant flies (n=16, vibrated; n=16, FR).

Note that, of the three genotypes shown here, only the antenna-ablated wildtype flies show a VS-shifted activity peak in FR after exposure to VS. We previously demonstrated that the *Drosophila* antennae, which contain thermal preference neurons and a large ChO (Johnston's organ) required for hearing (*4, 30, 31*), are not required for temperature synchronization of the circadian clock at the molecular and behavioral level (*2, 14*). Under the experimental conditions of this study wildtype flies without antennae even showed a more robust entrainment to VS cycles than their intact counterparts (see also Figs. 2B,C). Although we cannot rule out antennal contributions to clock synchronization by vibration, they are clearly not required- similar to what was reported for temperature entrainment (*2, 14*). Error bars represent SEM.

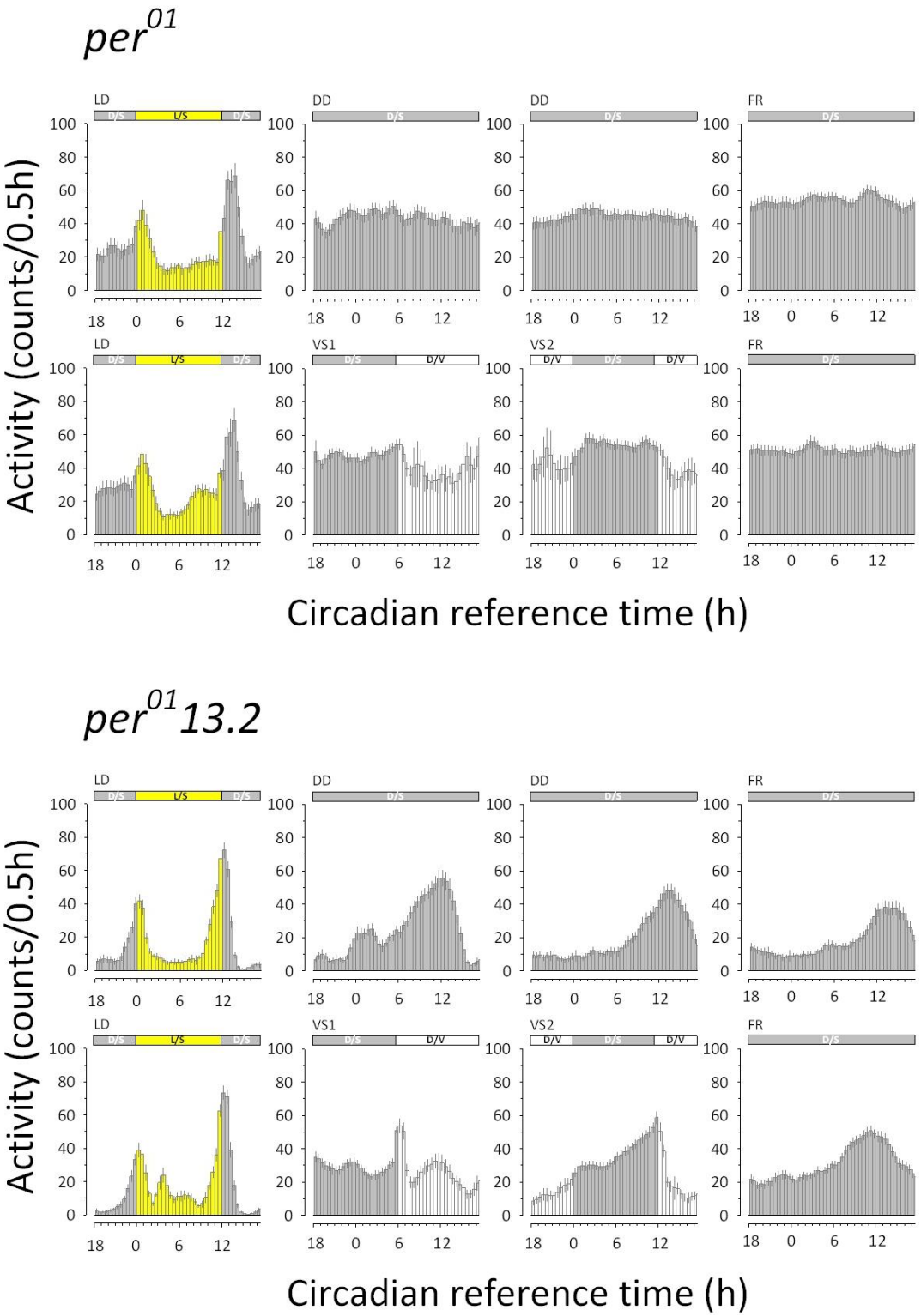

Fig. S6. Histograms showing the daily activity averages during four successive experimental stages of VS-exposed flies (LD→VS1→VS2→FR, bottom rows) and the corresponding phases of control flies (LD→DD→DD→ FR, top rows) for *per*^{01} mutants (n=32, vibrated, n=32, FR) and *per*^{01} *13.2* rescue

flies (n=16, vibrated, n=16, FR). Note that major activity peaks during the final free run (last histograms to the right) occur considerably after CT12 in the silent control but before CT12 in the VS-exposed flies, demonstrating entrainment to VS (see also Fig. 2). Error bars represent SEM.

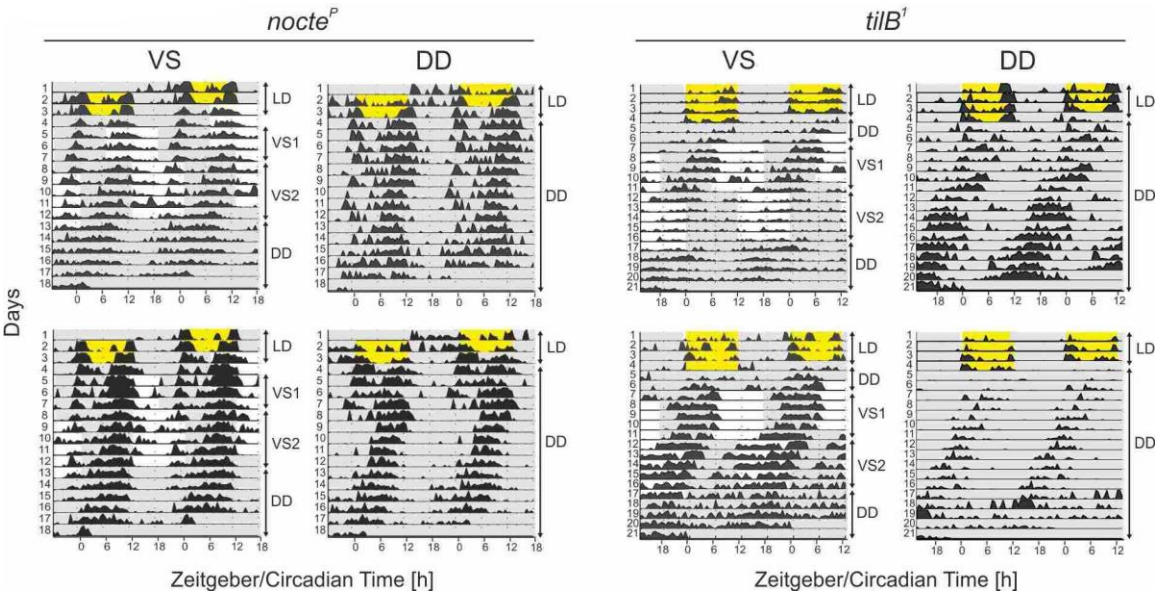

Fig. S7. Individual records of the indicated genotypes before, during and after mechanical stimulation. Individual actograms of flies exposed to the same VS conditions as in Fig. 2A are shown in the left columns (VS), controls not exposed to VS cycles are shown in the right columns (DD) for each genotype. All *nocte*^{P} and *tilB*^{1} mutant flies shown here were classified as 'not-synchronized'. See Table 1 for quantification of synchronized flies. Actogram shading as in Fig. 1C.

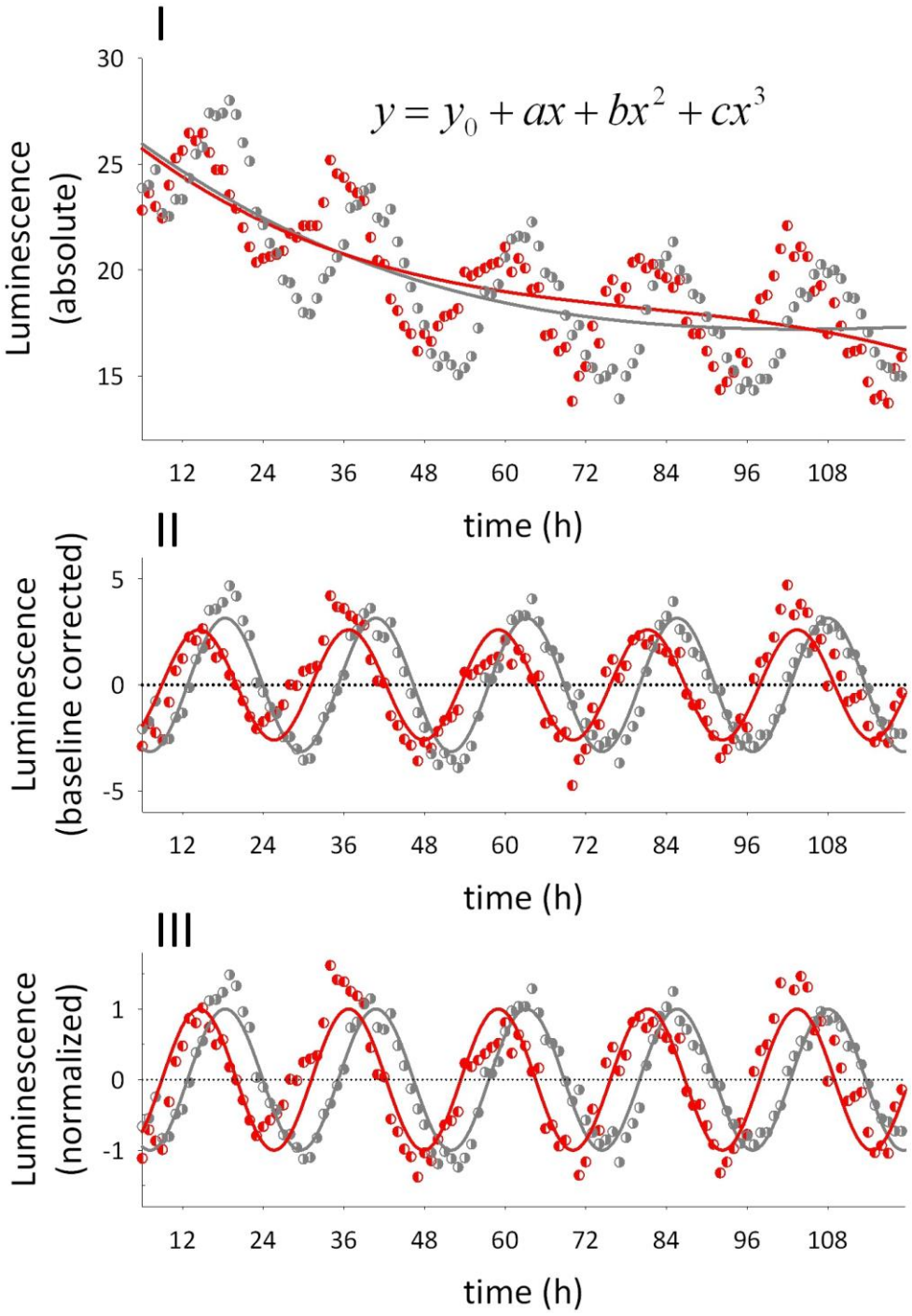

Fig. S8. Baseline-correction, sinusoidal modeling and phase analysis of bioluminescence data. (Top) baseline determination by fitting of a cubic polynomial to the raw data and subsequent subtraction of baseline resulting in de-trended, but otherwise unprocessed data. (Middle) fitting of a simple sinusoidal model to the de-trended data. (Bottom) Normalization of fit and data, highlighting phase differences. See supplemental text for further details.

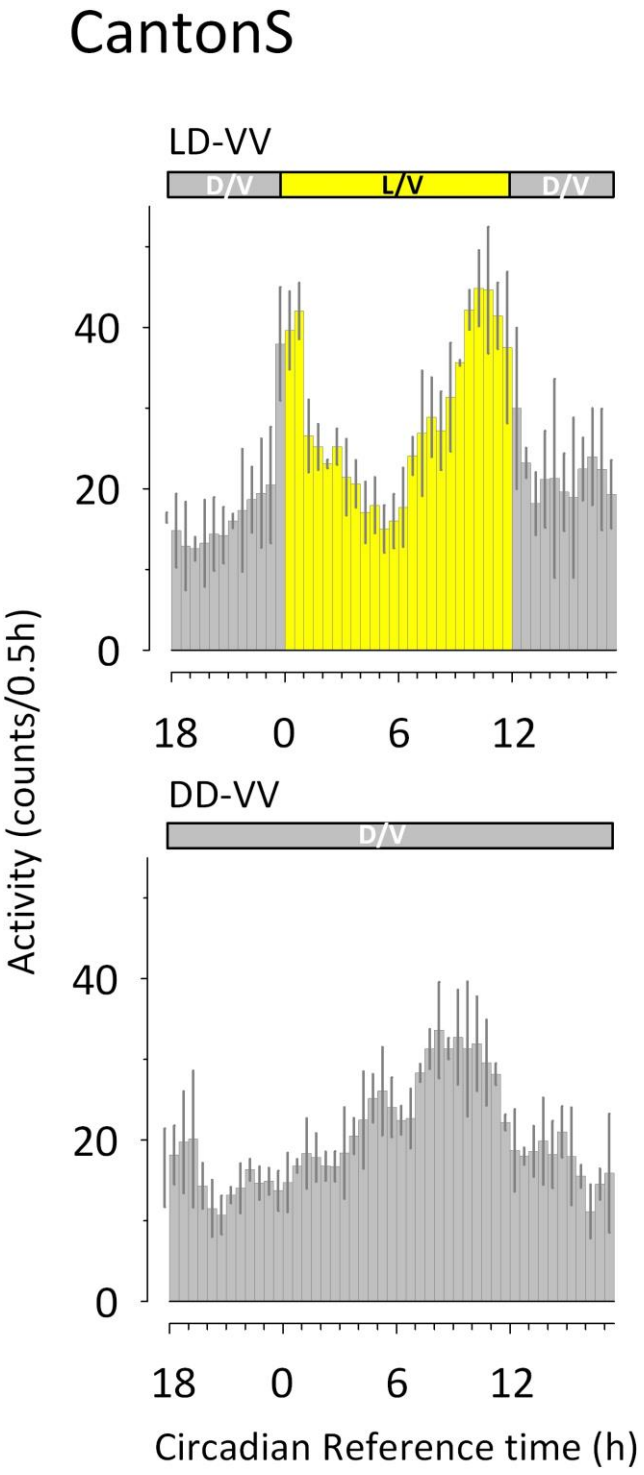

Fig. S9. Constant vibration does not disturb the pattern of locomotor activity in wildtype flies (CantonS). The vibratory stimulus sequence used for the VS entrainment experiments (see Fig. 1B) was played in constant loop (VV) to wildtype flies (CantonS, n=16), first during five consecutive 12h:12h LD cycles (LD-VV, yellow areas mark the 'light ON' phases) and then in complete darkness (DD-VV). Daily average activity of the flies is plotted for the LD+VV (top) and the DD+VV (bottom) part. Note that a continuous (i.e. not diurnally patterned) vibration, by itself, does not affect the

characteristic activity pattern, or activity levels, resulting from LD-entrainment (both during the actual entrainment phase as well as the following free-run). Error bars represent SEM.

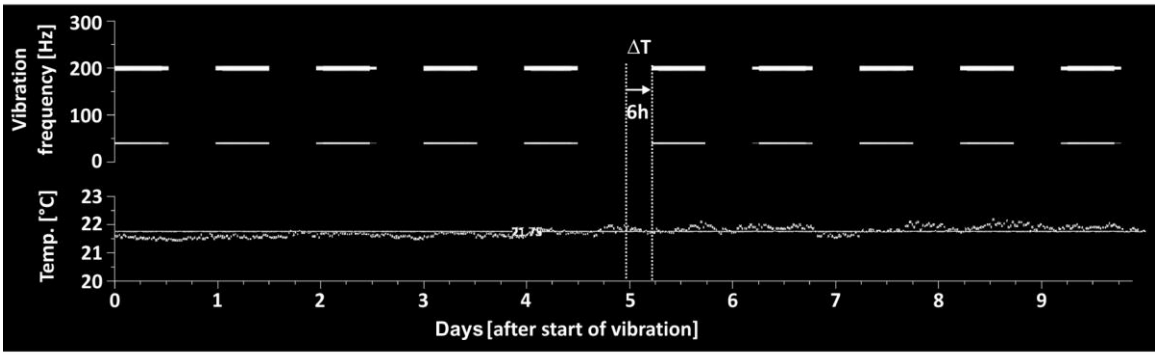

Fig. S10. Temperature and vibrations were monitored during the entire course of each VS entrainment. The figure shows 9 consecutive days of a representative experiment. The upper panel shows a sonogram of the 12h:12h, vibration/silence stimulus. The vibration stimulus consisted of a 40Hz component, which alternated with a 200Hz component (see also Fig. 1B). The lower panel shows the minimal temperature fluctuations that accompanied the VS experiment. All VS entrainment experiments were carried out in complete darkness. Note the 6h shift of vibration stimulus (ΔT) at day 5.

Table S1. Summary of vibration experiments involving the genotypes indicated in the left column. 'n' total number of individuals tested for each genotype. '% entrained' indicates flies that were judged as having synchronized to the VS cycles after 'genotype-blind' inspection of individual actograms. 'τ' indicates free running (DD + silence) period (± SEM) and '% rhythmic' the percentage of flies with RS values ≥1.5. (see ref. (*7*) for details). 'Δ Phase' indicates the difference of the average peak activity phase during the final free-running portion (5 days) of each experiment between VS flies and control flies kept in DD and silence after LD entrainment (S). ns: not significant, na: not applicable.

	Flies exposed to vibration (VS)				Flies kept in silence (S)			Δ Phase (h)
genotype	n	% entrained	τ (h)	% rhythmic	n	τ (h)	% rhythmic	
CantonS	312	53.3	23.9 ± 0.1	71.0	155	24.0 ± 0.1	93.8	4.9 ± 0.3
CantonS(w/o antennae)	52	73.6	24.0 ± 0.1	83.3	41	23.9 ± 0.1	95.1	6.5
per^{01}	31	2.1	23.7 ± 0.2	6.5	32	23.1 ± 0.5	15.6	na
per^{01}*; 13.2*	16	71.4	23.9 ± 0.1	94.0	18	24.0 ± 0.1	66.7	2.1
nocte^{P}	16	0	23.8 ± 0.2	68.8	16	23.6 ± 0.1	100	ns
tilB^{1}	24	12.6	23.0 ± 0.5	50	26	23.2 ± 0.1	84.6	ns

References (complete, for main text and supplement):

1. S. Panda, J. B. Hogenesch, S. A. Kay, *Nature* **417**, 329 (May, 2002).
2. H. Sehadova *et al.*, *Neuron* **64**, 251 (Oct, 2009).
3. L. H. Field, T. Matheson, in *Advances in Insect Physiology, Vol 27*. (Academic Press Inc, San Diego, 1998), vol. 27, pp. 1-228.
4. M. J. Kernan, *Pflugers Archiv-European Journal of Physiology* **454**, 703 (Aug, 2007).
5. F. T. Glaser, R. Stanewsky, *Cold Spring Harb. Symp. Quant. Biol.* **72**, 233 (2007).
6. M. J. Hamblen-Coyle, D. A. Wheeler, J. E. Rutila, M. Rosbash, J. C. Hall, *J. Insect Behav.* **5**, 417 (1992).
7. Materials and methods are available as supplementary materials on Science Online.
8. C. Gentile, H. Sehadova, A. Simoni, C. H. Chen, R. Stanewsky, *Curr. Biol.* **23**, 185 (Feb 4, 2013).
9. J. D. Levine, P. Funes, H. B. Dowse, J. C. Hall, *Bmc Neurosci* **3**, (Jan 18, 2002).
10. R. J. Konopka, S. Benzer, *Proc Natl Acad Sci U S A* **68**, 2112 (Sep, 1971).
11. Y. Citri *et al.*, *Nature* **326**, 42 (Mar 5-11, 1987).
12. D. M. Zerr, J. C. Hall, M. Rosbash, K. K. Siwicki, *J Neurosci* **10**, 2749 (Aug, 1990).
13. R. G. Kavlie, M. J. Kernan, D. F. Eberl, *Genetics* **185**, 177 (May, 2010).
14. F. T. Glaser, R. Stanewsky, *Curr Biol* **15**, 1352 (Aug 9, 2005).
15. S. Veleri, C. Brandes, C. Helfrich-Forster, J. C. Hall, R. Stanewsky, *Curr. Biol.* **13**, 1758 (Oct 14, 2003).
16. D. A. Golombek, R. E. Rosenstein, *Physiological Reviews* **90**, 1063 (Jul, 2010).
17. N. Mrosovsky, *Biol. Rev. Camb. Philos. Soc.* **71**, 343 (Aug, 1996).
18. R. E. Mistlberger, D. J. Skene, *Biol. Rev.* **79**, 533 (Aug, 2004).
19. J. D. Levine, P. Funes, H. B. Dowse, J. C. Hall, *Science* **298**, 2010 (Dec, 2002).
20. F. W. Turek, S. Loseeolson, *Nature* **321**, 167 (May 8, 1986).
21. W. F. Zimmerman, C. S. Pittendrigh, T. Pavlidis, *J. Insect Physiol.* **14**, 669 (1968).
22. K. A. Stokkan, S. Yamazaki, H. Tei, Y. Sakaki, M. Menaker, *Science* **291**, 490 (Jan, 2001).
23. N. Mrosovsky, P. A. Salmon, *Nature* **330**, 372 (Nov 26, 1987).
24. F. van Oosterhout *et al.*, *PLoS ONE* **7**, e39693 (2012).
25. N. Mrosovsky, P. A. Salmon, *Chronobiol. Int.* **7**, 35 (Jan 1, 1990).
26. A. Kamikouchi, J. T. Albert, M. C. Göpfert, *Eur. J. Neurosci.* **31**, 697 (Feb, 2010).
27. R. J. Gegear, A. Casselman, S. Waddell, S. M. Reppert, *Nature* **454**, 1014 (2008).
28. T. Yoshii, M. Ahmad, C. Helfrich-Förster, *PLoS Biol.* **7**, e1000086 (2009).
29. W. Wolfgang, A. Simoni, C. Gentile, R. Stanewsky, *Proceedings of the Royal Society B: Biological Sciences* **280**, (October 7, 2013).
30. M. Gallio, T. A. Ofstad, L. J. Macpherson, J. W. Wang, C. S. Zuker, *Cell* **144**, 614 (2011).
31. O. Sayeed, S. Benzer, *Proc Natl Acad Sci U S A* **93**, 6079 (Jun 11, 1996).